Reviving the Energy Independent Soln. of the Solar Neutrino Anomaly

S. Choubey, S. Goswami, N. Gupta & DPR

hep-ph/0103318, Phys Rev. (in press)

Long History: Acker, Pakvasa, Learned, Weiler PL '93

Harrison, Perkins, Scott PL '95, '96

Fogli & Volkas hep-ph/9510312

Acker & Pakvasa PL '97

Conforto et al. PL '98

Scott NP (Proc. Suppl.) '98,

hep-ph/0010335

Why Energy Independent Soln?

1. Energy Independent Day/Night Spectrum SK

2. Bi Maximal Mixing Models of ν Mass Matrix

Niv '00

Grossman, Niv, Shadmi '98

Barbieri, Hall, Smith, Strumia, Weiner '98

$\epsilon = \cos 2\theta = 1 - 2\sin^2\theta$

$\epsilon \sim 2m_e/m_\mu \sim .01$

$\sim \delta m^2_{12}/\delta m^2_{13} \lesssim .01$

$\sim \delta m_{12}/\delta m_{13} \lesssim .1$

$\Rightarrow \lesssim 10\%$ Energy Dep. in the Ga-SK range

Not Measurable Exbt.ly

Solar ν (Expts.)

S.T. Petcov
hep-ph/9806466

Non monotonic energy dep. ⇒ SMA MSW or Vac. Osc.

$\langle P_{\nu_e \to \nu_e} \rangle$ 0.57 0.33 0.46 (0.36) St (Ac)

SSM (BP)

$f_B = 5.15 \times 10^6 / cm^2/sec$ $(1.0 \pm {}^{.20}_{.16})$

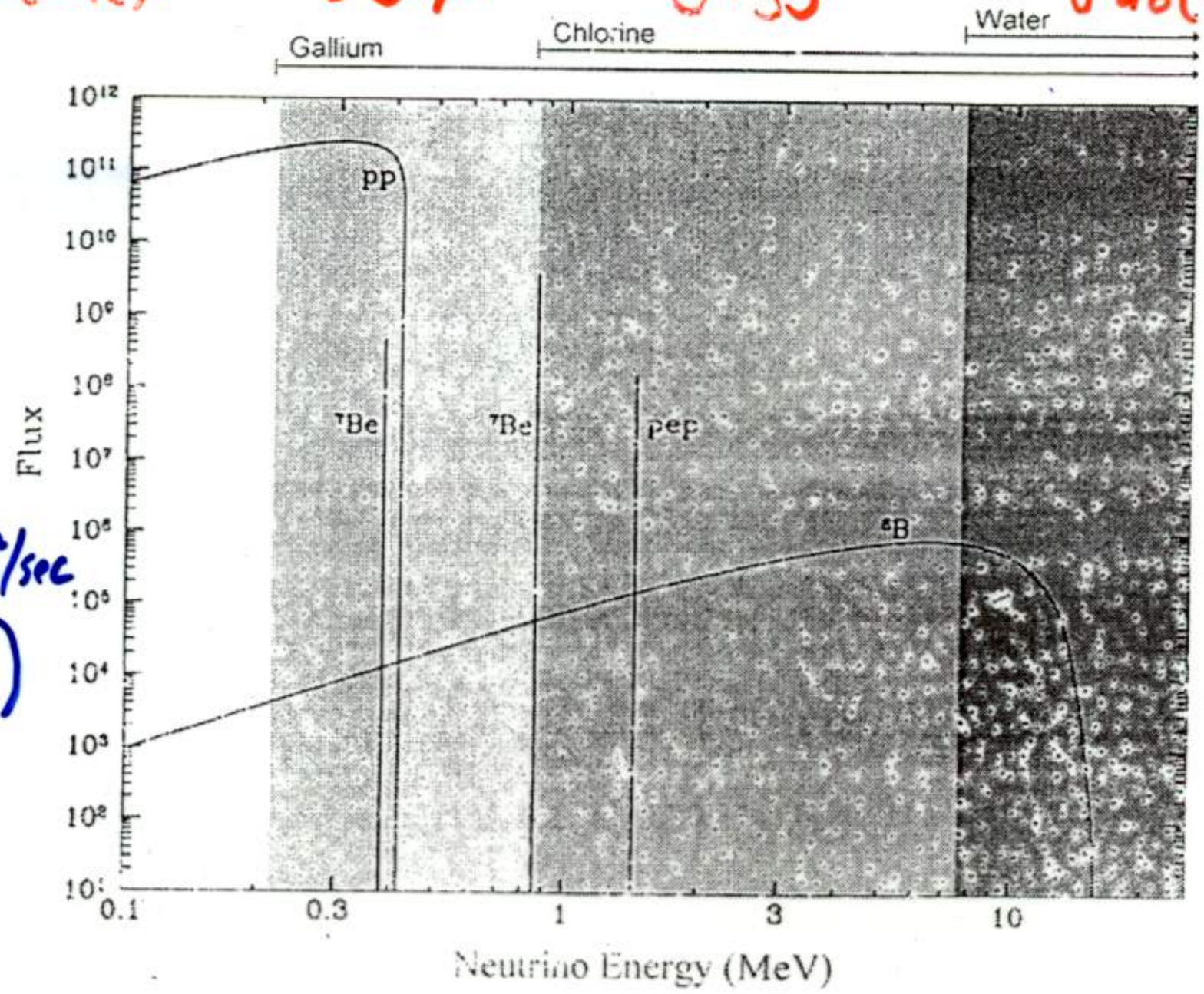

Fig. 2. The spectra of the pp, pep, ^{7}Be and ^{8}B neutrino fluxes (from [23]). Shown are also the ranges of solar neutrino energies to which the Ga - Ge, Cl - Ar and Kamiokande II and III experiments are sensitive.

GALLEX/CNO
SAGE
Ga: $\nu_e + {}^{71}Ga \to e^- + {}^{71}Ge$ } Radiochemical separation of ^{71}Ge & ^{37}Ar

Homestake (Davis et al.) Cl: $\nu_e + {}^{37}Cl \to e^- + {}^{37}Ar$

S.K/Kamioka $\nu_e + e^- \xrightarrow{CC} e^- + \nu_e$ Water Cerenkov
$(\nu_\mu + e^- \xrightarrow{NC} e^- + \nu_\mu)$ Real time Directionality

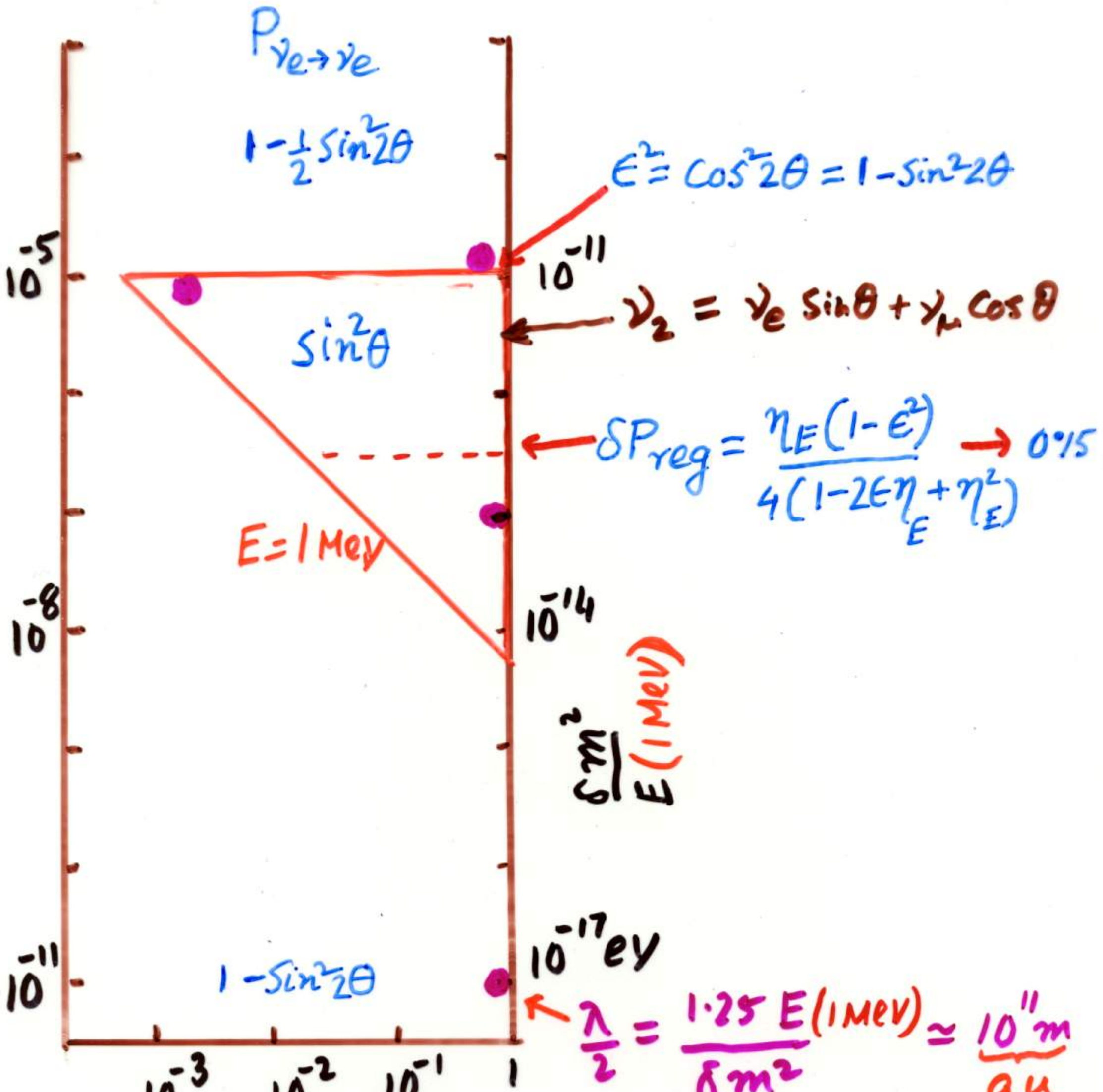

$$\eta_E = 0.66 \left(\frac{\delta m^2/E}{10^{-13}\, ev} \right) \frac{1}{\rho\, Ye}$$

ρ = Earth Density in g/cm^3

Ye = No of electrons per Nucleon

Ga 1
E<1 ↑
>1 ↓0
SK
1

$\frac{1+\epsilon^2}{2}$
Ga ↑
SK ↓ $\frac{1-\epsilon}{2}$

Ga ↑ E<1
SK ↓ >1

E<1 ↑
E^2
↓
E>1

Gonzalez-Garcia & Pena Garay
NP Supl. 2000

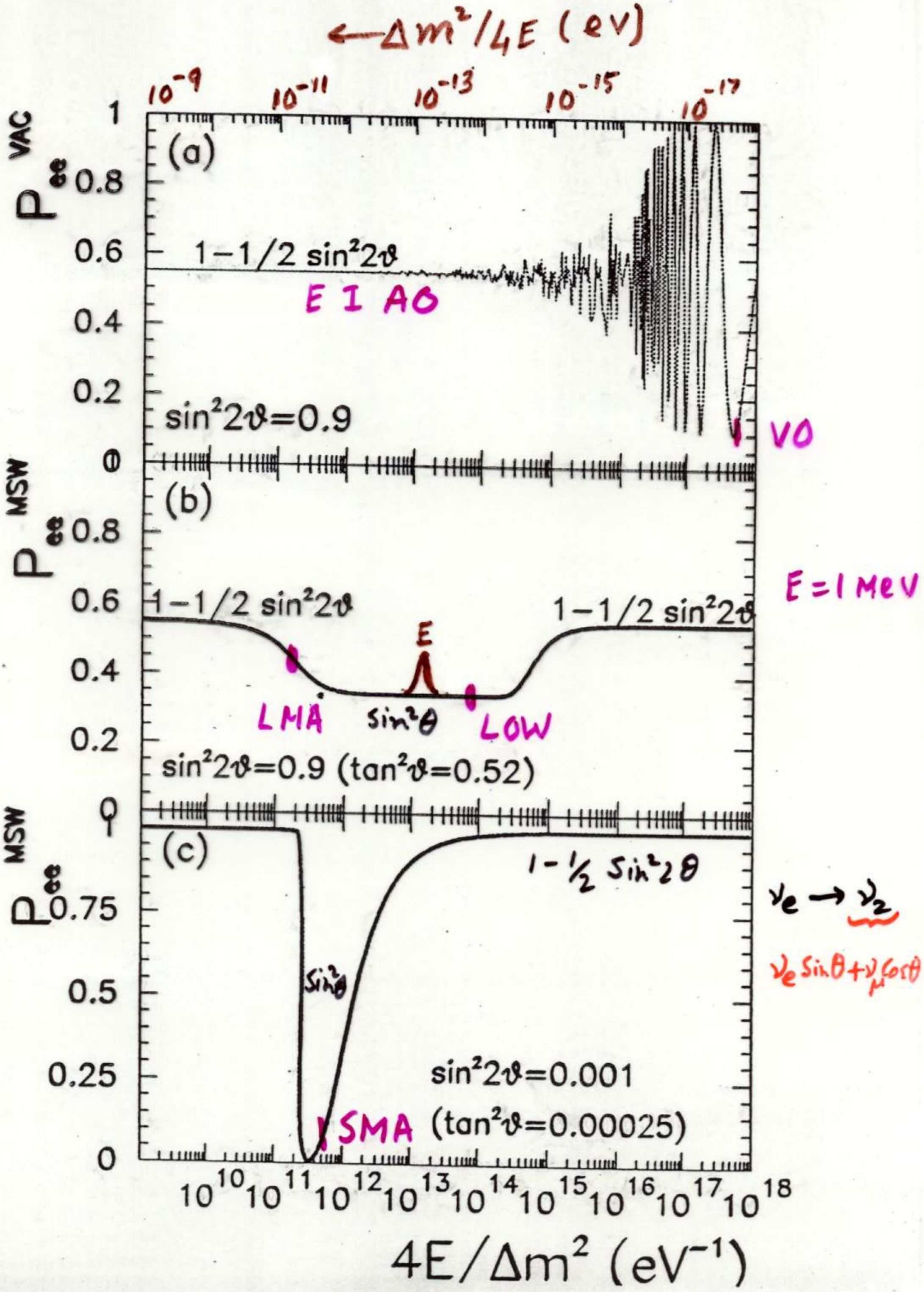

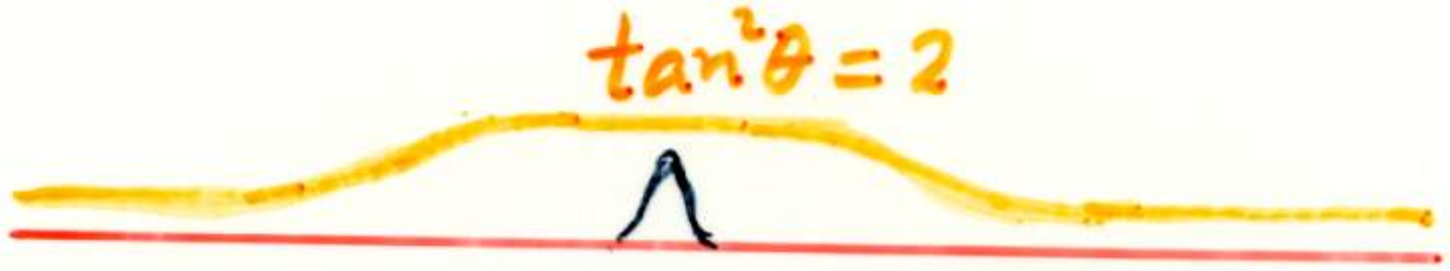
$\tan^2\theta = 2$
$\tan^2\theta = 1$
EI

Spectrum Ratio to the SSM prediction

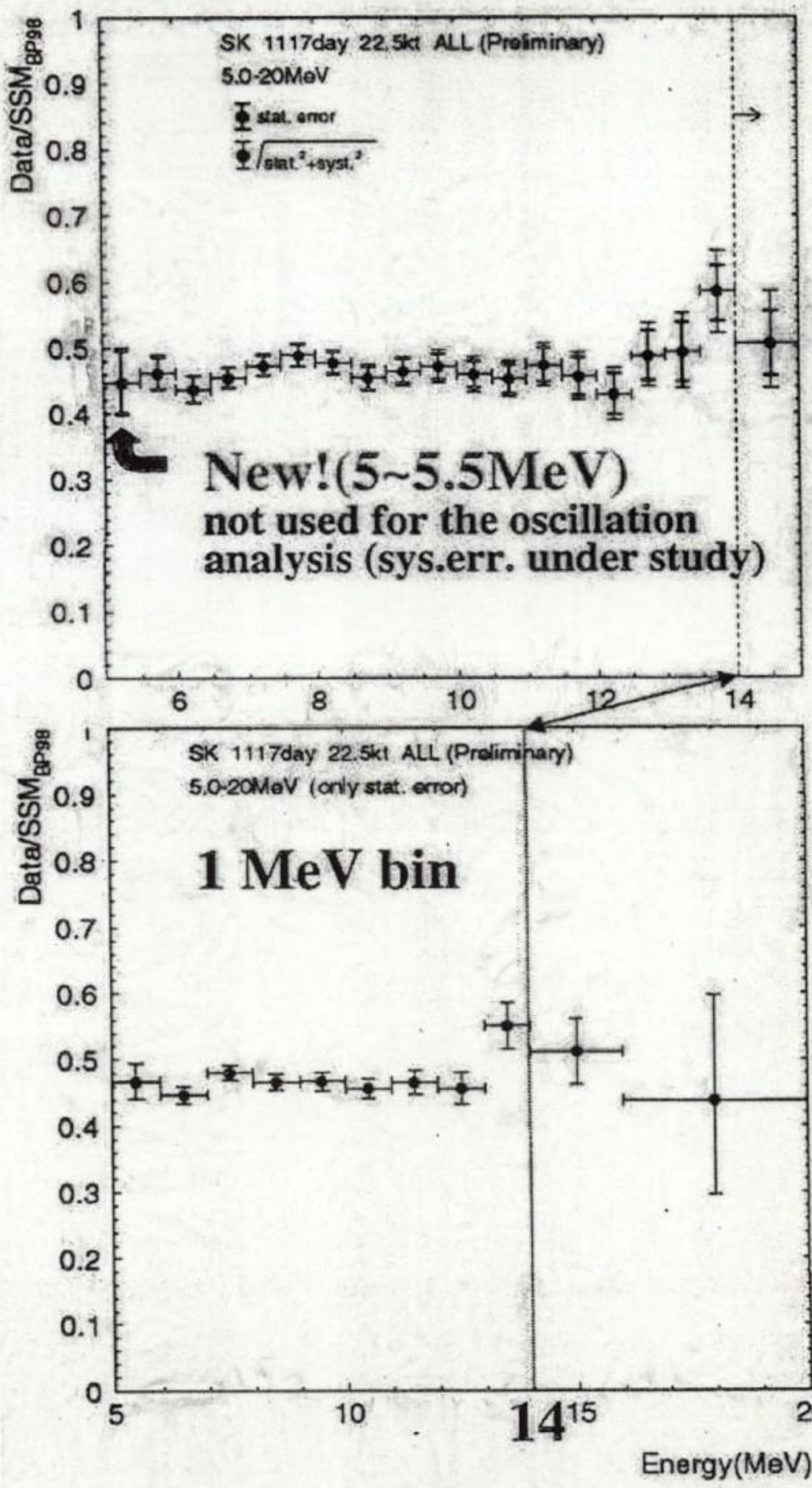

χ^2 for flat :
13.7 / 17dof
(69% C.L.)
incl. sys. err.

Consistent to be flat.

Day/Night Flux difference

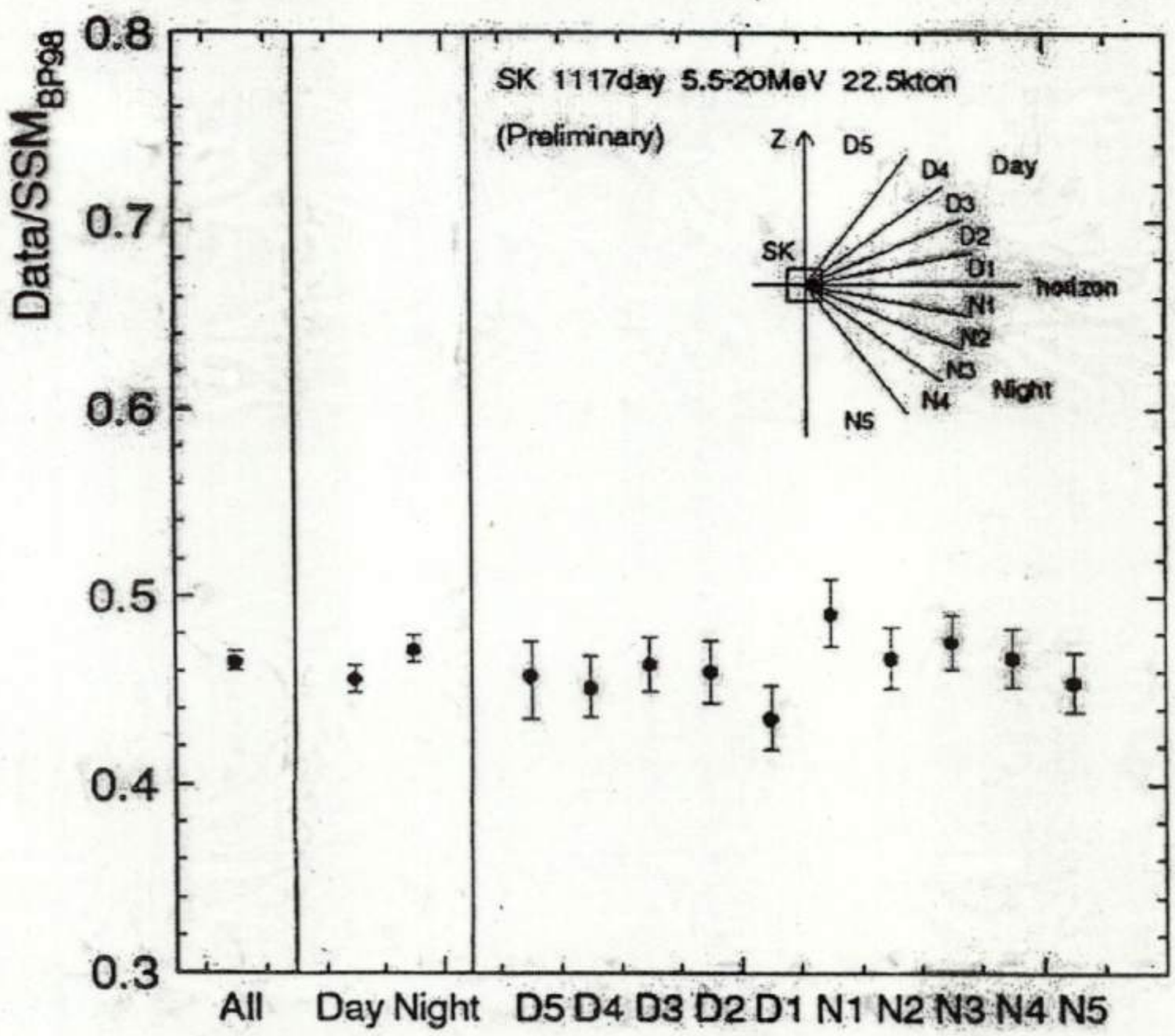

$$\text{Day} = 2.35 \pm 0.04(\text{stat.}) \pm^{0.08}_{0.07}(\text{syst.})\ \text{x}10^6/\text{cm}^2/\text{s}$$

$$\text{Night} = 2.43 \pm 0.04(\text{stat.}) \pm^{0.08}_{0.07}(\text{syst.})\ \text{x}10^6/\text{cm}^2/\text{s}$$

$$\frac{\text{D-N}}{\text{(D+N)/2}} = -0.034 \pm 0.022(\text{stat.})\ ^{+0.013}_{-0.012}\ (\text{syst.})$$

1.3 σ level → not strong yet

$\nu_e \longrightarrow \nu_\mu$ oscillation (95% C.L.)

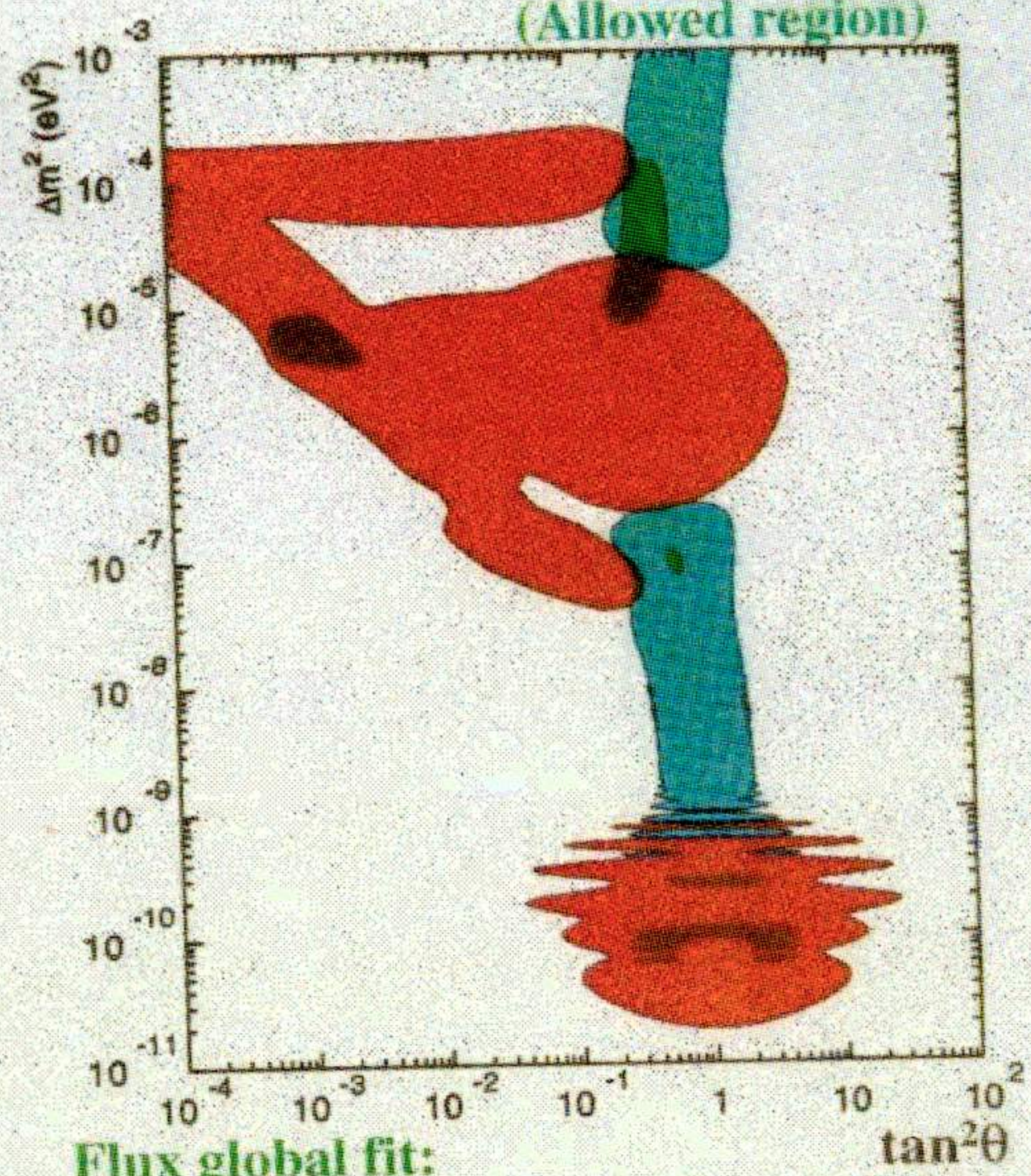

Flux global fit:
Ga+Cl+SKflux
(Allowed region)

Super-Kamiokande only
Day/Night Spectrum
(flux independent)
(Excluded region)

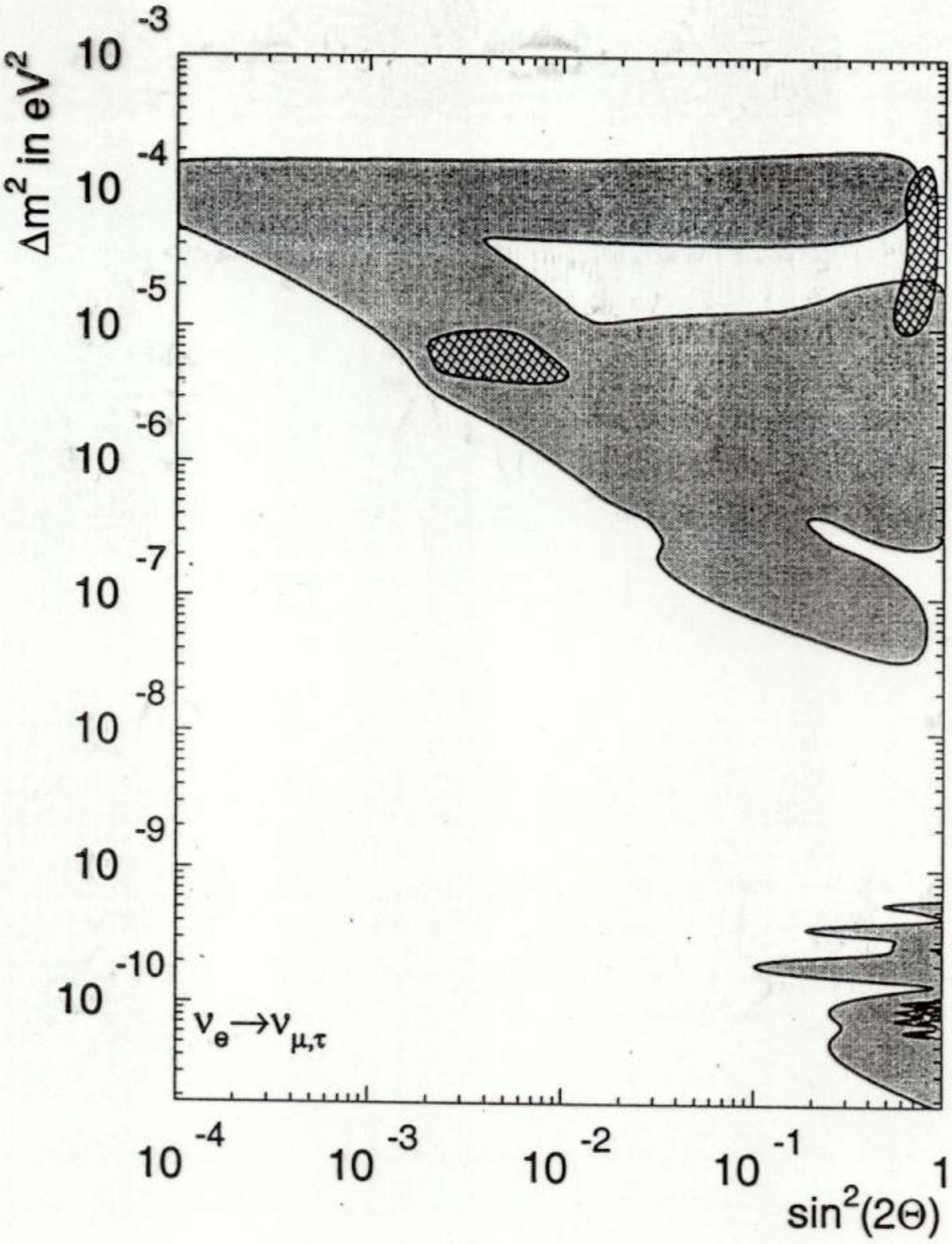

FIG. 4: Exclusion area for two-flavor oscillation $\nu_e \leftrightarrow \nu_\mu/\nu_\tau$ from a day/night spectrum analysis. The hatched area is allowed at 95%C.L. by the combined flux analysis same as in Fig. 2

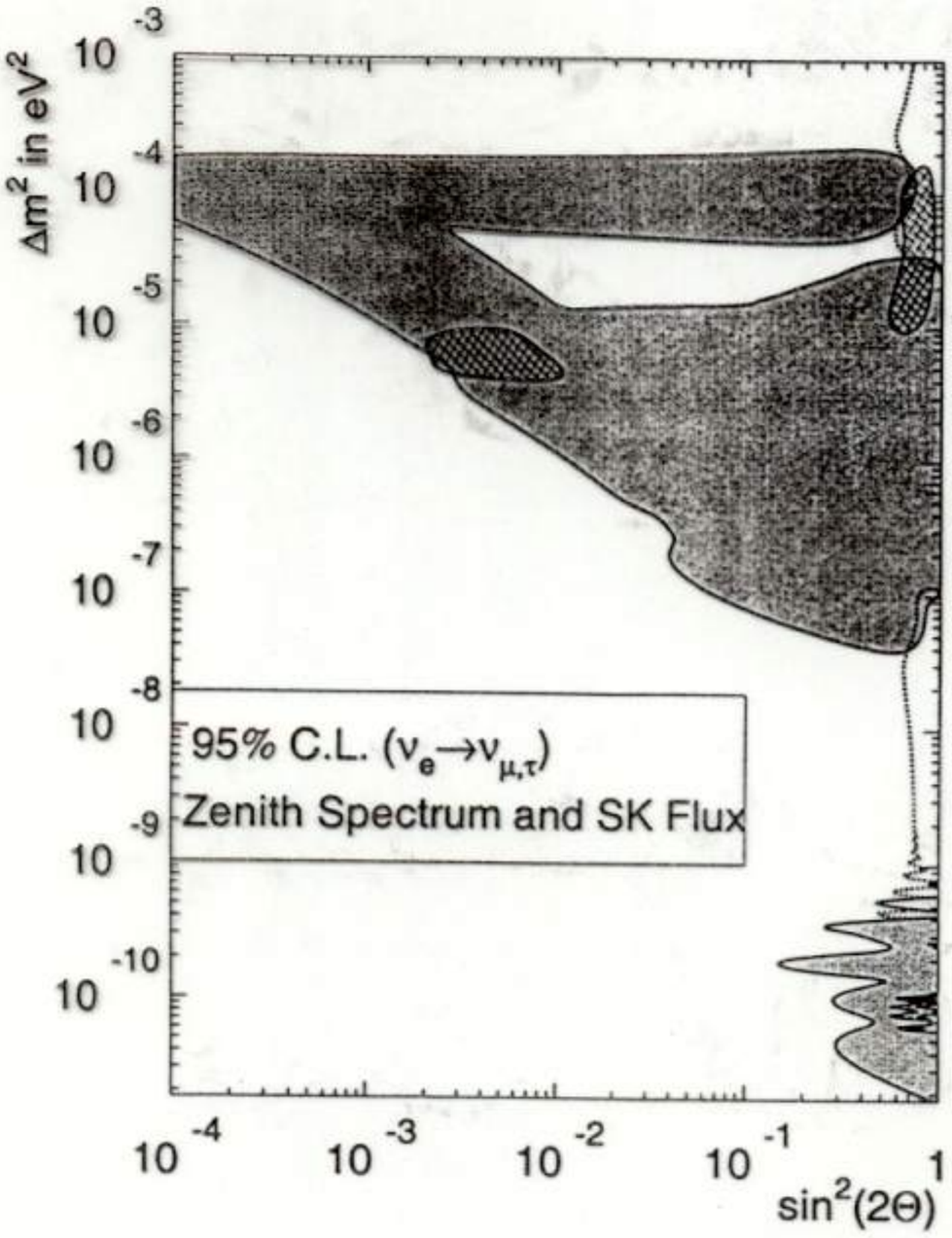

FIG. 2: Exclusion area for two-flavor oscillation $\nu_e \leftrightarrow \nu_\mu/\nu_\tau$ from zenith angle spectrum analysis at 95% confidence level. Overlaid are the allowed areas (95% C.L.) using the zenith angle spectrum and the SSM flux prediction (dotted lines). The small overlap of allowed area and excluded area is due to the fairly good agreement of the flux for these parameters. The hatched areas are allowed at 95% in a combined fit to the fluxes measured at GALLEX[4], SAGE[3], Homestake[1] and Super-Kamiokande[5]

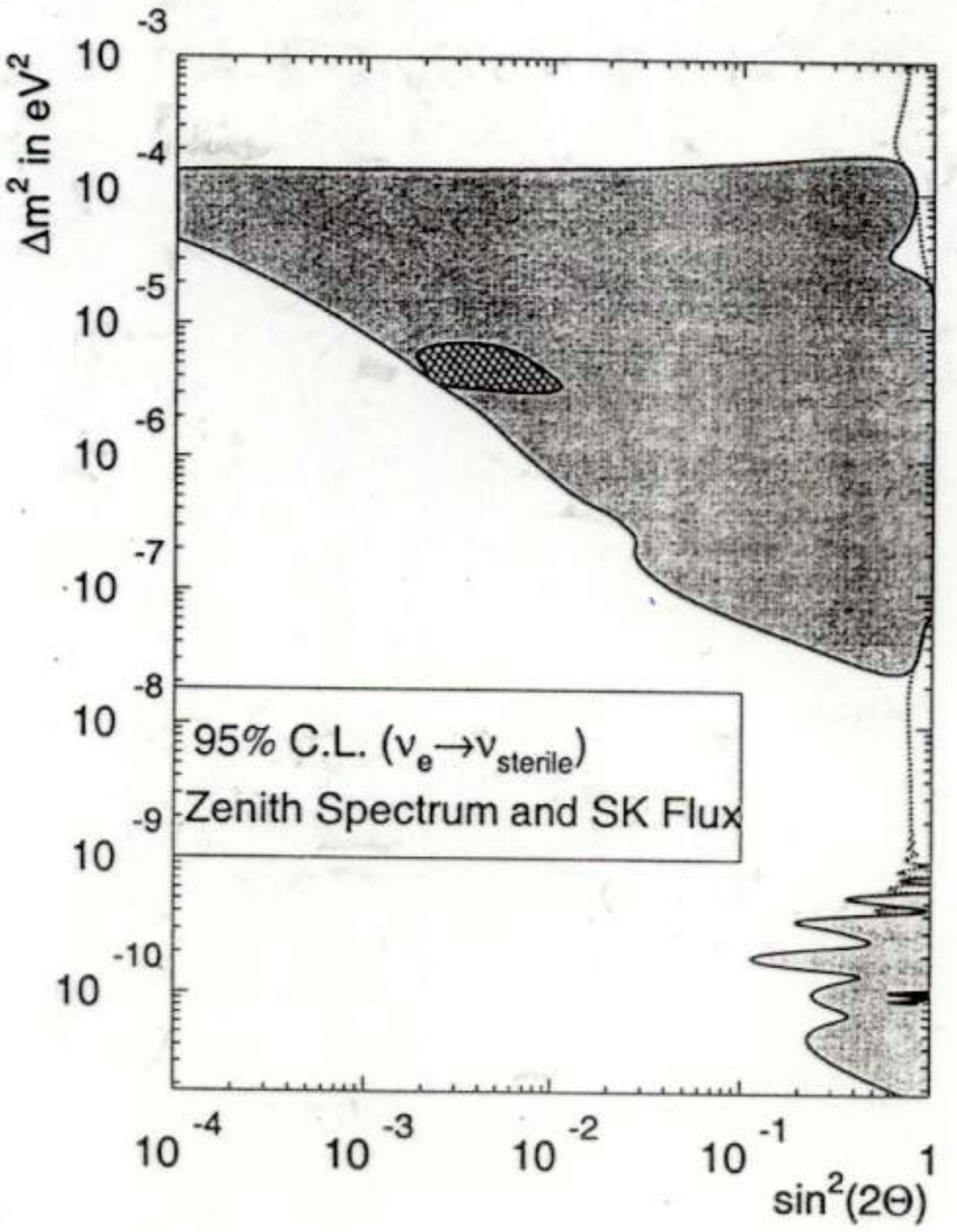

FIG. 3: Exclusion area for two-flavor oscillation $\nu_e \leftrightarrow \nu_{\text{sterile}}$ from zenith angle spectrum analysis at 95% confidence level. Overlaid are the allowed areas (95% C.L.) using the zenith angle spectrum and the SSM flux prediction (dotted lines). The hatched areas are allowed at 95% in a combined fit to the fluxes measured at GALLEX[4] and SAGE[3], Homestake[1] and Super-Kamiokande[5].

Experiment	Gallium	Clorine	SuperKamiokanda
Suppr. Rate Data/SSM BP	0.576 ± 0.04	0.327 ± 0.029	0.465 ± 0.015 $(0.36 \pm .015)$
E_{th} (MeV)	0.2	0.8	6.5
Composition	pp (55%), Be (25%), B (10%)	B (75%), Be (15%)	B (100%)

1. Upward Renorm. of Cl Data by 20%. (2σ)

$\longrightarrow 0.39 \pm .03$

$\because$ Cl expt. not calibrated

& SK Spectra $\Rightarrow$ Monotonic Energy Dependence

LMA & LOW $\Rightarrow$ Cl $\gtrsim$ SK

2. Downward Renorm. of BP ^8B ν flux

$f_{BP} = 5.15 \times 10^6 \, cm^{-2} sec^{-1} \left(1.0 \, {}^{+.20}_{-.16}\right)$

by 25 % (1.5σ)

$\because$ ^8B flux very sensitive to Solar Model Par.

& Helio seismic Models favour lower ^8B ν flux

$f \simeq 3.2 \times 10^6$ Brun Turck-Chieze Morel APJ '98

$f = (4 \pm 0.3) \times 10^6$ Antia, Chitre, Goswami, Kar '00

Brun, Antia, Chitre '01

$$P = 1 - \frac{1}{2}\sin^2 2\theta$$

	Nature of Solution	X_B	$\sin^2 2\theta \begin{pmatrix} \tan^2\theta \\ \text{or} \\ \cot^2\theta \end{pmatrix}$	$\chi^2_{\min}$	Goodness of fit
Chlorine Observed	Active	1.0	0.95(0.63)	46.15	14.39%
		0.77	0.96(0.68)	45.86	12.25%
	Sterile	1.0	0.89(0.52)	53.66	3.75%
		0.83	0.92(0.57)	54.63	2.55%
Chlorine Renormalised	Active	1.0	0.89(0.52)	37.65	43.13%
		0.73	0.88(0.50)	36.05	46.63%
	Sterile	1.0	0.85(0.44)	40.89	30.35%
		0.79	0.85(0.44)	40.09	26.4%

Table 2: The best-fit value of the parameter, the $\chi^2_{\min}$ and the g.o.f from a combined analysis of rate and spectrum with the energy independent solution (2).

$$\chi^2 = \sum_{i,j} (F_i^{th} - F_i^{exp})(\sigma_{ij}^{-2})(F_j^{th} - F_j^{exp})$$

Exptl. & Theoretical errors (SSM)

g.o.f = Prob. of a Correct Model having $\chi^2 > \chi^2_{min}$

$$= \frac{1}{\Gamma(N/2)} \int_{\frac{\chi^2_{min}}{2}}^{\infty} e^{-t} t^{\frac{N}{2}-1} dt$$

N = d.o.f

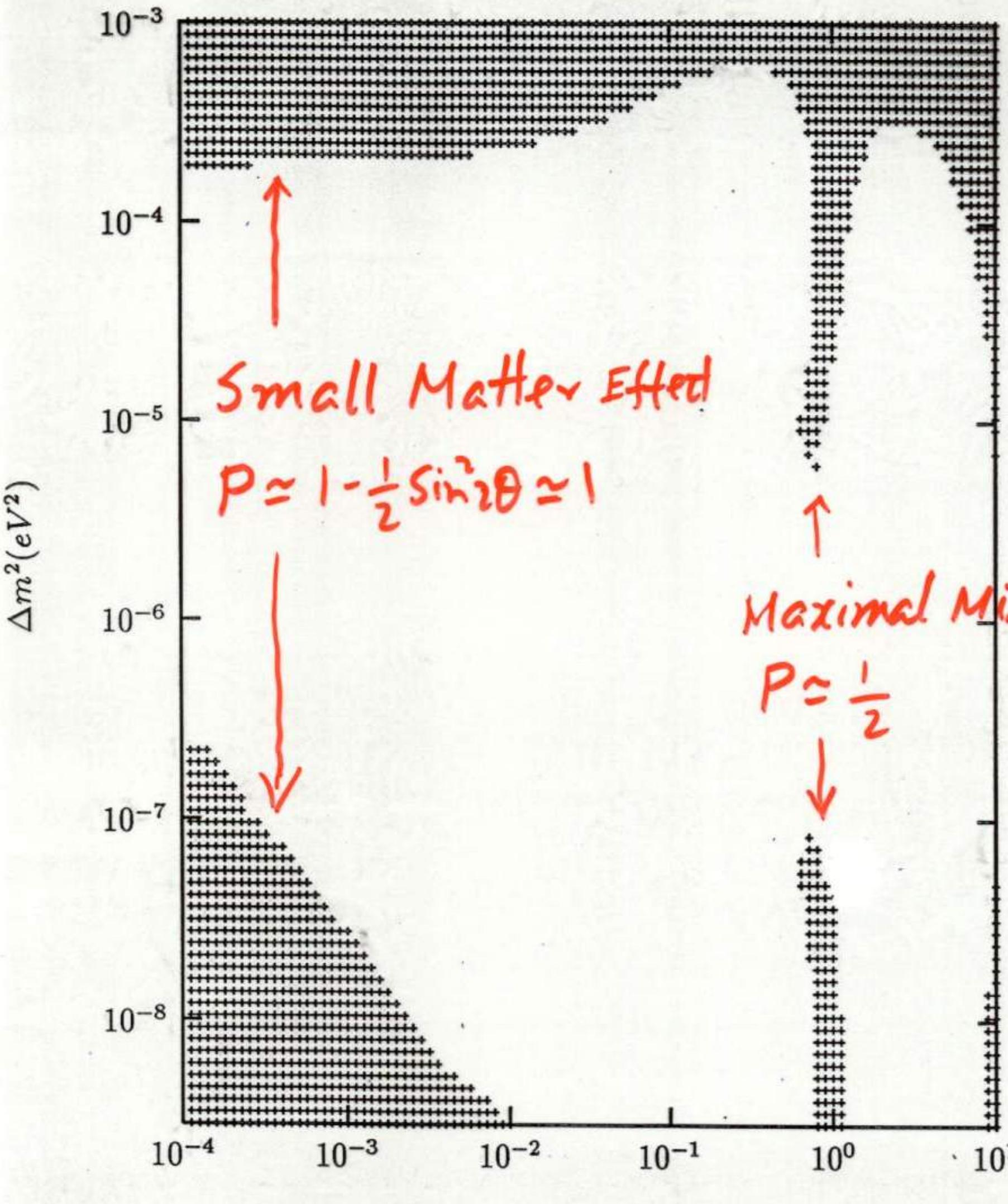

Effectively Energy Independent Region
($P \simeq 1 - \frac{1}{2}\sin^2 2\theta$ within 10%
over the Ga-SK energy range)

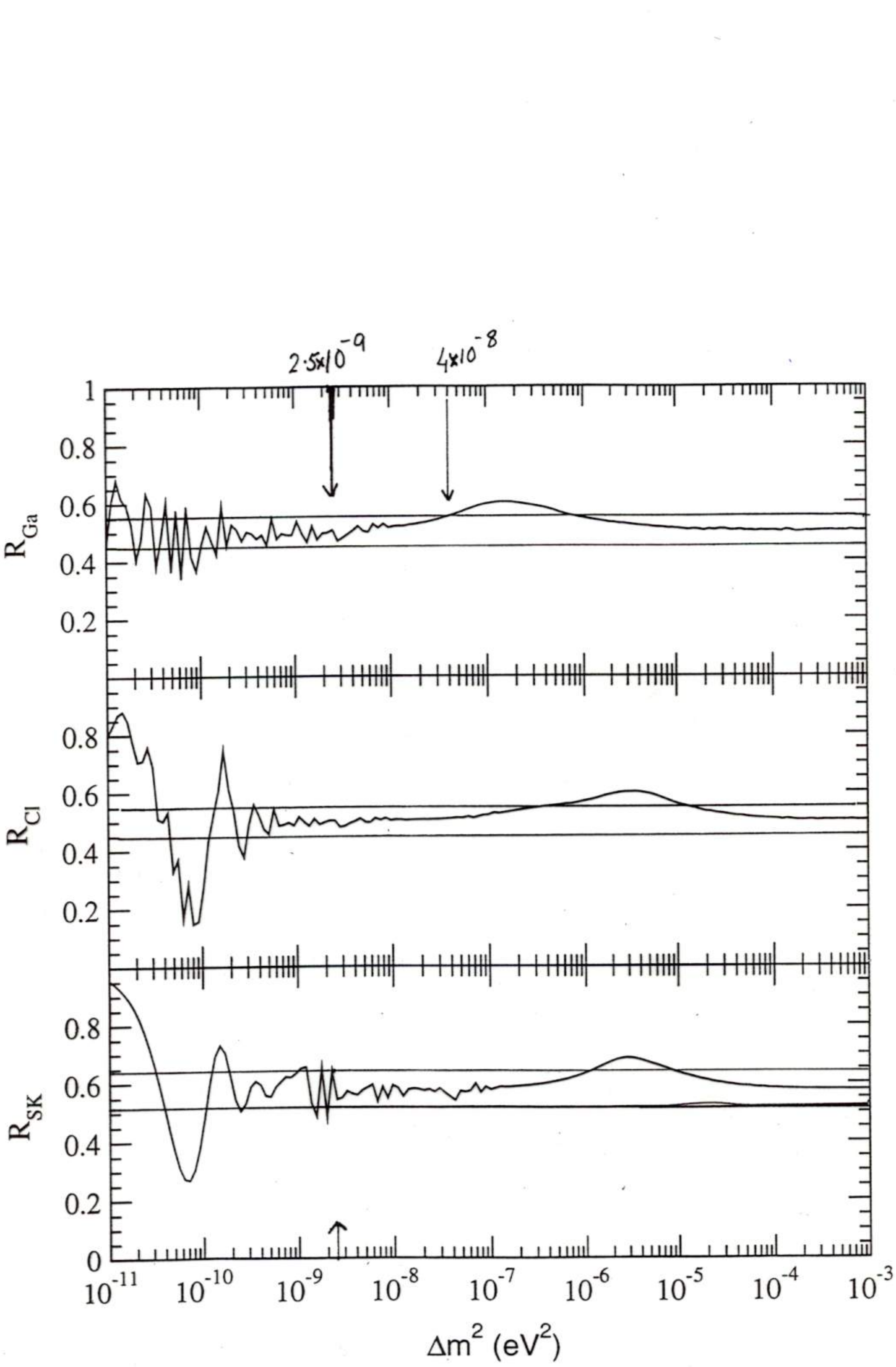
2.5×10^{-9}
4×10^{-8}
R_{Ga}
R_{Cl}
R_{SK}
1
0.8
0.6
0.4
0.2
0
10^{-11}
10^{-10}
10^{-9}
10^{-8}
10^{-7}
10^{-6}
10^{-5}
10^{-4}
10^{-3}
Δm^2 (eV^2)

	Type of Neutrino	Nature of Solution	Δm^2 in eV^2	$tan^2\theta$	χ^2_{min}	g.o.f
Cl Obsvd.	Active	SMA	5.48×10^{-6}	5.79×10^{-4}	43.22	19.01%
		LMA	4.18×10^{-5}	0.36	37.33	40.78%
		LOW	1.51×10^{-7}	0.64	39.54	31.48%
	Sterile	SMA	3.74×10^{-6}	5.2×10^{-4}	44.85	14.79%
		LMA	1.03×10^{-4}	0.58	52.18	3.96%
		LOW	3.47×10^{-8}	0.82	50.57	5.43%
Cl Renorm.	Active	SMA	4.97×10^{-6}	3.15×10^{-4}	42.43	21.37%
		LMA	6.68×10^{-5}	0.39	30.32	73.53%
		LOW	1.63×10^{-7}	0.76	32.43	63.9%
	Sterile	SMA	3.44×10^{-6}	3.59×10^{-4}	41.98	22.76%
		LMA	1.04×10^{-4}	0.53	37.9	38.27%
		LOW	4.08×10^{-8}	0.84	36.8	42.98%

Table 3: The best-fit values of the parameters, the χ^2_{min} and the g.o.f from a combined analysis of rate and spectrum in terms of ν_e oscillation into an active/sterile neutrino, including the matter effects.

Cl observed ⇒ Acceptable LMA & LOW Solns
but not SMA.
No acceptable sterile soln.

Cl Renorm ⇒ Much better LMA & LOW solns
but not SMA.

Sterile LMA & LOW solns
poorer than the active ones.

90 %., 95 %. & 99 %.CL Allowed Regions

Limited Overlap with

Energy Ind. (Max. Mixing) Region

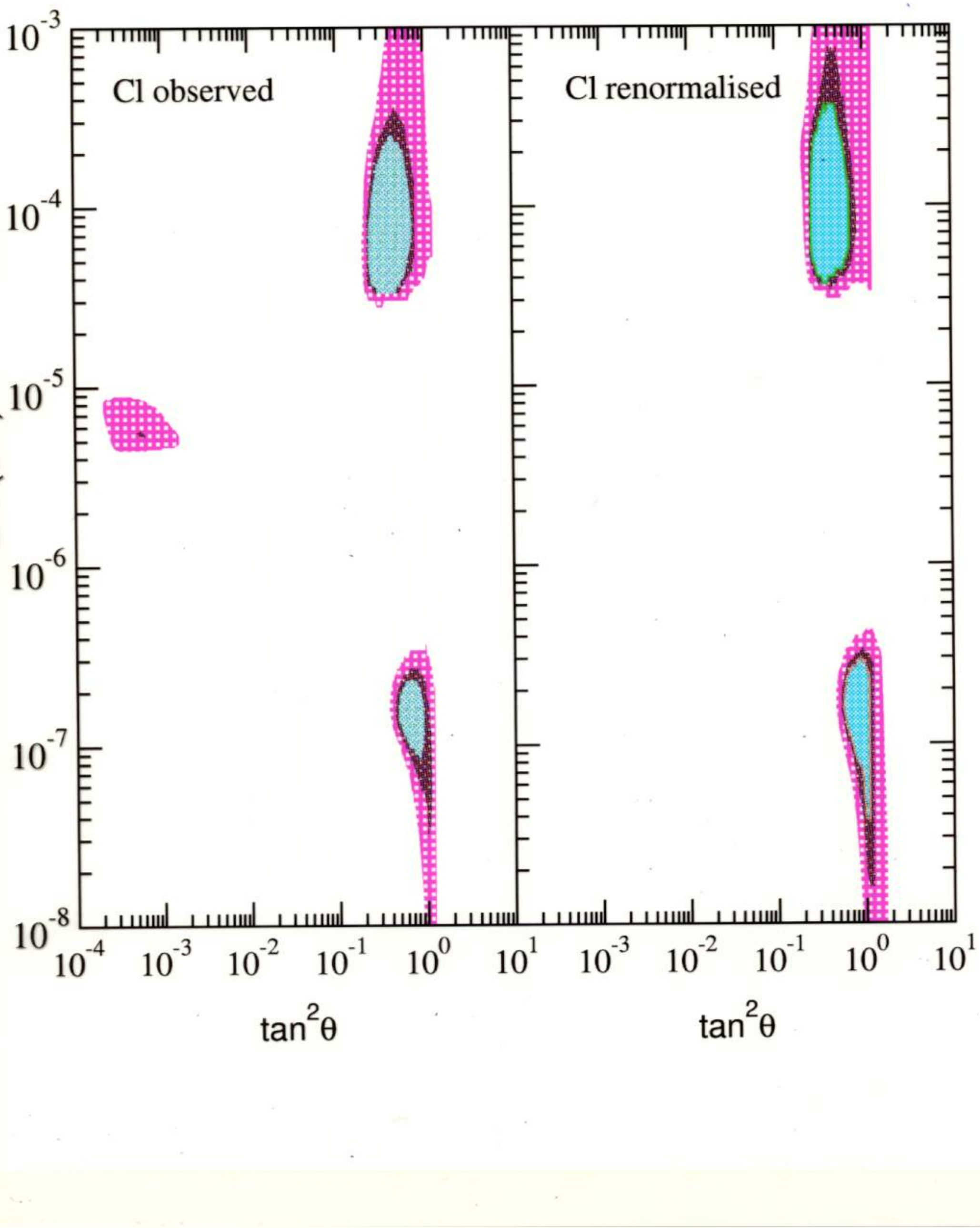

		Nature of Solution	Δm^2 in eV^2	$tan^2\theta$	χ^2_{min}	g.o.f
Cl Obsvd.	$X_B = 0.75$	SMA	5.43×10^{-6}	5.09×10^{-4}	39.50	31.64%
		LMA	4.39×10^{-5}	0.54	43.18	19.13%
		LOW	1.41×10^{-7}	0.69	41.88	23.08%
	0.57 X_B 1.34 0.93	SMA	5.35×10^{-6}	4.35×10^{-4}	37.98	37.92%
		LMA	4.21×10^{-5}	0.25	34.22	55.34%
		LOW	1.51×10^{-7}	0.63	39.59	31.28%
Cl Renorm.	$X_B = 0.75$	SMA	4.95×10^{-6}	3.11×10^{-4}	38.15	37.19%
		LMA	6.92×10^{-5}	0.57	34.06	56.11%
		LOW	1.59×10^{-7}	0.82	32.76	62.35%
	0.53 X_B 1.14 0.88	SMA	4.90×10^{-6}	2.92×10^{-4}	35.57	48.89%
		LMA	6.57×10^{-5}	0.35	29.94	75.14%
		LOW	1.64×10^{-7}	0.76	31.95	66.17%

Table 4: Best fits to the combined rates and spectrum data in terms of ν_e oscillation into active neutrino with $X_B = 0.75$ and free X_B.

$X_B = 0.75 \Rightarrow$ Enhances SK rate more than the Cl.

Cl Observed $\Rightarrow$ Accentuates rise between Cl $\rightarrow$ SK rates.

$\Rightarrow$ Favours SMA over LMA & LOW soln.

Cl Renorm. $\Rightarrow$ LMA & LOW much better than SMA

g.o.f much better than Cl observed

& much larger allowed range in Param. Space

free X_B: $X_B > 1$ Suppresses SK rate more than Cl.

$\Rightarrow$ Favoured by LMA Soln.

$\Rightarrow$ Accentuates energy dependence between Ga & SK rates

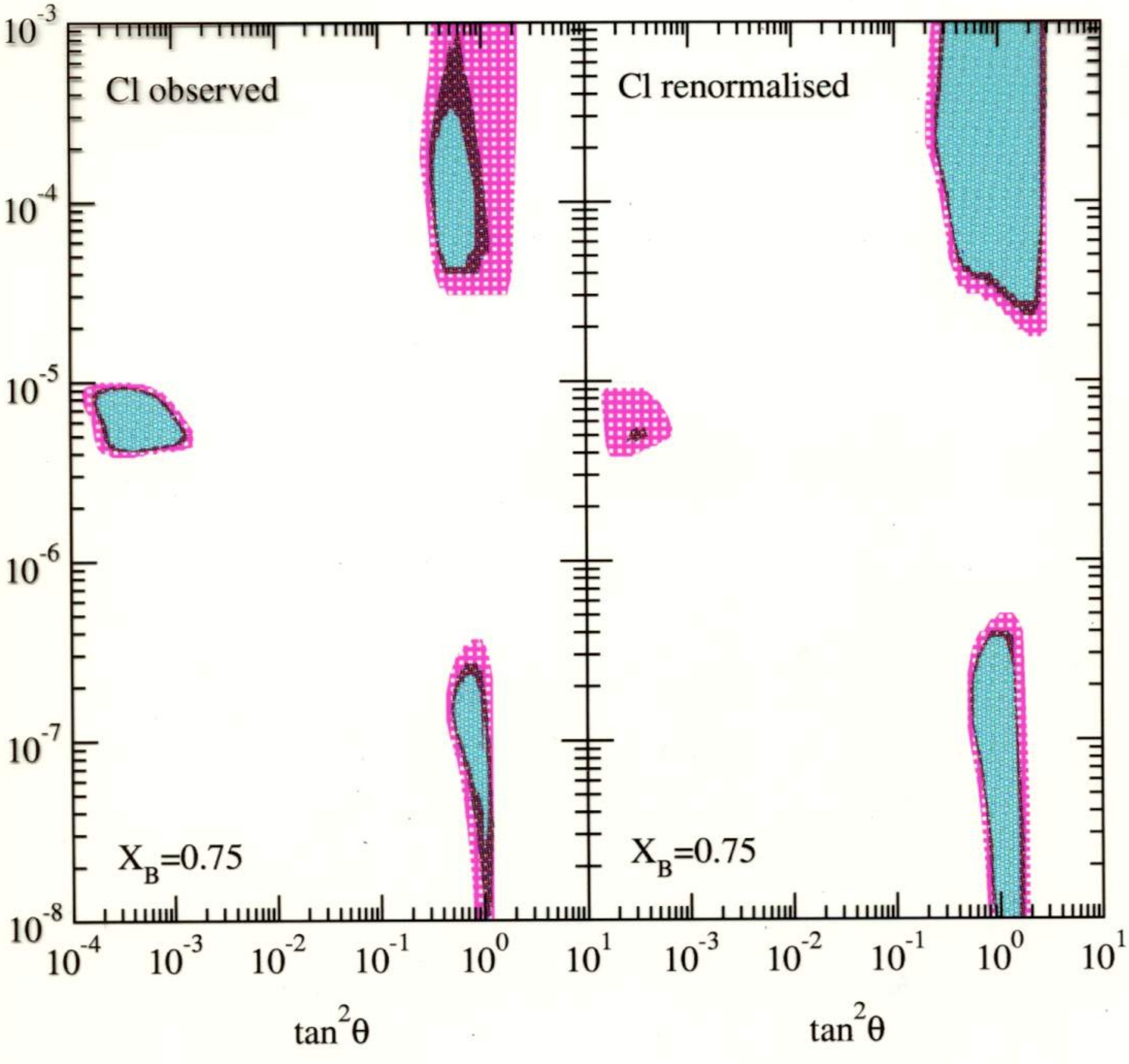

Much of the enlarged range of the LMA & LOW Solns encompases the energy independent (Max Mixing) region.

Nature of Solution	Δm^2	$tan^2\theta$	R_{cc}/R_{nc}
LMA	6.68×10^{-5}	0.39	0.32
LOW	1.63×10^{-7}	0.76	0.45
energy independent	-	0.52	0.55

$1.75 \pm .14 / 5.4 \pm 1$

$\sigma \rightarrow 4\ \%$

Table 5. The R_{cc}/R_{nc} at SNO at the best-fit values for the LMA, LOW and energy independent solution for the renormalised Chlorine and X_B fixed cases of Table 2 and Table 3.

$(X_B = 1)$

^8B flux factors out from the ratio cc/nc.

SNO energy range $\simeq$ SK

$\therefore$ Compare energy dependent model(LMA, LOW) predictions for this: $R_{cc}/R_{nc} < 0.5$

with the energy independent model prediction: $R_{cc}/R_{nc} \geq 0.5$

$\frac{1-\epsilon}{2}$ $\frac{1+\epsilon^2}{2}$

—

LMA Soln $\Rightarrow$ Oscillatory behavior for KamLAND reactor $\bar{\nu}$ data.

—

LOW Soln $\Rightarrow$ Large D/N Assym. $> 10\%$ for Be ν @ KamLAND & Borexino.

old [5] this derived flux difference is $0.53 \pm 0.17 \times 10^6$ $cm^{-2}s^{-1}$, or 3.1σ. The probability that this difference is not a downward fluctuation is 99.87%. These data are therefore evidence of a non-electron active flavor component in the solar neutrino flux. These data are also inconsistent with the "Just-So^2" parameters for neutrino oscillation [15].

Figure 3 displays the inferred flux of non-electron flavor active neutrinos ($\phi(\nu_{\mu\tau})$) against the flux of electron neutrinos. The two data bands represent the one standard deviation measurements of the SNO CC rate and the Super-Kamiokande ES rate. The error ellipses represent the 68%, 95%, and 99% joint probability contours for $\phi(\nu_e)$ and $(\phi(\nu_{\mu\tau}))$. The best fit to $\phi(\nu_{\mu\tau})$ is:

$$\phi(\nu_{\mu\tau}) = 3.69 \pm 1.13 \times 10^6 \text{ cm}^{-2}\text{s}^{-1}.$$

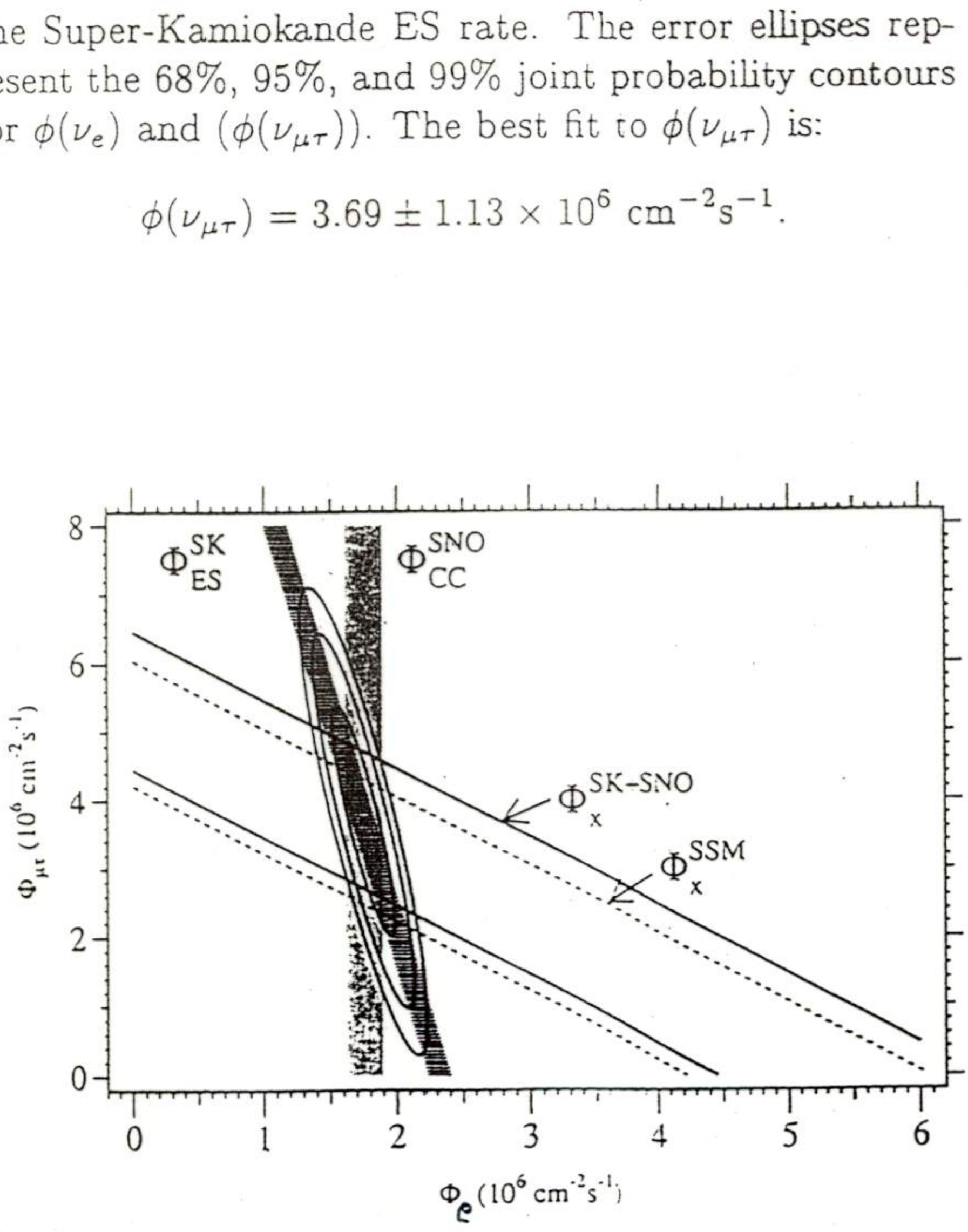

ses [16,15] limits on and $\Delta m^2_{\mu\tau}$ the sum o 0.05 and 8 $< \Omega_\nu <$ (critical de

In sum direct ind the solar n of the tot

This re Sciences a Industry (Northern Province Energy, a gineering Astronom vided by I (AECL), tronics C Telecom a ter was lo Power Ge

* Decea
† Perma Vancc
‡ Perma don, I
§ Perma Chilto Susse

Phys Rev D. (in press)

TIFR/TH/01-07
SINP/TNP/01-07

Reviving the energy independent suppression of the solar neutrino flux

Sandhya Choubey[a], Srubabati Goswami[a], Nayantara Gupta[b], D.P. Roy[c]

[a] Saha Institute of Nuclear Physics,
1/AF, Bidhannagar, Calcutta 700 064, INDIA
[b] Indian Association for the Cultivation of Sciences
Calcutta 700 032, INDIA
[c] Tata Institute of Fundamental Research
Homi Bhabha Road, Mumbai 400 005, INDIA

Abstract

We explore the possibility of an energy independent suppression of the solar neutrino flux in the context of the recent SuperKamiokande data. From a global analysis of the rate and spectrum data, this scenario is allowed at only 14% probability with the observed Cl rate. If we allow for a 20% upward renormalisation of the Cl rate along with a downward renormalisation of the B neutrino flux then the fit improves considerably to a probability of $\sim$ 50%. We compare the quality of these fits with those of the MSW solutions. These renormalisations are also found to improve the quality of the fits with MSW solutions and enlarge the allowed region of their validity in the parameter space substantially. Over much of this enlarged region the matter effects on the suppression of the solar neutrino flux are found to be very weak, so that the solutions become practically energy independent.